Hydrothermal sediments as a potential record of seawater Nd isotope compositions: The Rainbow vent site (36°14′N, Mid-Atlantic Ridge)

Valérie Chavagnac,[1] Martin R. Palmer,[2] J. Andrew Milton,[2] Darryl R. H. Green,[1] and Christopher R. German[1,3]

Received 19 January 2006; revised 18 May 2006; accepted 31 May 2006; published 9 September 2006.

[1] Geochemical compositions and Sr and Nd isotopes were measured in two cores collected ~2 and 5 km from the Rainbow hydrothermal vent site on the Mid-Atlantic Ridge. Overall, the cores record enrichments in Fe and other metals from hydrothermal fallout, but sequential dissolution of the sediments allows discrimination between a leach phase (easily leachable) and a residue phase (refractory). The oxy-anion and transition metal distribution combined with rare earth element (REE) patterns suggest that (1) the leach fraction is a mixture of biogenic carbonate and hydrothermal Fe-Mn oxy-hydroxide with no significant contribution from detrital material and (2) >99.5% of the REE content of the leach fraction is of seawater origin. In addition, the leach fraction has an average $^{87}Sr/^{86}Sr$ ratio indistinguishable from modern seawater at 0.70916. Although we lack the ε_{Nd} value of present-day deep water at the Rainbow vent site, we believe that the REE budget of the leach fraction is predominantly of seawater origin. We suggest therefore that the leach fraction provides a record of local seawater ε_{Nd} values. Nd isotope data from these cores span the period of 4–14 ka (^{14}C ages) and yield ε_{Nd} values for North East Atlantic Deep Water (NEADW) that are higher (−9.3 to −11.1) than those observed in the nearby Madeira Abyssal Plain from the same depth (−12.4 ± 0.9). This observation suggests that either the Iceland-Scotland Overflow Water (ISOW) and Lower Deep Water contributions to the formation of NEADW are higher along the Mid-Atlantic Ridge than in the surrounding basins or that the relative proportion of ISOW was higher during this period than is observed today. This study indicates that hydrothermal sediments have the potential to provide a higher-resolution record of deep water ε_{Nd} values, and hence deepwater circulation patterns in the oceans, than is possible from other types of sediments.

Citation: Chavagnac, V., M. R. Palmer, J. A. Milton, D. R. H. Green, and C. R. German (2006), Hydrothermal sediments as a potential record of seawater Nd isotope compositions: The Rainbow vent site (36°14′N, Mid-Atlantic Ridge), *Paleoceanography*, *21*, PA3012, doi:10.1029/2006PA001273.

1. Introduction

[2] Many studies have shown that major oceanic water masses are characterized by distinct Nd isotope ratios (referred to as ε_{Nd} values) [e.g., *Piepgras and Wasserburg*, 1987]. Hence studies of phases that record the ε_{Nd} value of seawater (e.g., Fe-Mn nodules and crusts) can be used in paleoceanographic studies; for example, *David et al.* [2001] used ε_{Nd} values of Fe-Mn crusts to track changes in weathering inputs to the Pacific Ocean over the past 26 Myr. It would be useful to apply ε_{Nd} studies to more recent periods, such as glacial-interglacial intervals, but Fe-Mn crusts and nodules grow too slowly and most other phases (e.g., carbonates) that might record seawater ε_{Nd} values have Nd concentrations that are generally low. High-quality data on such material can only be acquired after an extensive and careful cleaning of the foraminifera and chemical separation, which is highly time-consuming and prone to high analytical blanks. In this study, we suggest that rapidly accumulating hydrothermal sediments have the potential to provide high-resolution records of seawater ε_{Nd} values without these analytical problems.

[3] Hydrothermal systems are a widespread feature of mid-ocean ridges and represent the expulsion of high-temperature fluids at the seafloor. These fluids percolate through and cool the oceanic crust, before rising from vent chimneys to mix turbulently with the surrounding seawater. As dilution progresses, a range of polymetallic particles are formed and are either deposited near the vent-orifice or advected laterally by bottom currents away from the source region. Much of the Fe in hydrothermal fluids precipitates as sulfides within a few meters of the vent site, with the remaining Fe forming oxy-hydroxide complexes that scavenge and uptake dissolved elements (including Nd) from seawater as they precipitate and fall to the seafloor [e.g., *German et al.*, 2002]. These hydrothermal sediments accumulate at several cm per kyr

[1]National Oceanography Centre, Southampton, University of Southampton, Southampton, UK.
[2]School of Ocean and Earth Sciences, University of Southampton, Southampton, UK.
[3]Now at Department of Geology and Geophysics, Woods Hole Oceanographic Institution, Woods Hole, Massachusetts, USA.

0883-8305/06/2006PA001273$12.00

[*Cave et al.*, 2002]; hence they have the potential to provide high-resolution records of seawater ε_{Nd} values.

2. Previous Studies

[4] Reconstruction of water mass distributions and flow patterns in the ocean through the past cannot rely on the classic oceanographic tools of temperature, salinity and nutrient concentrations because none of this information is available directly from the geologic record. Instead, that information is deduced from geochemical and isotopic proxies. Radiogenic isotope ratios of trace metals dissolved in seawater are independent of fractionation induced by biological processes (see *Frank* [2002] for review) and therefore represent ideal tools with which to evaluate the strength of thermohaline circulation and to assess the extent of ocean-margin interactions over glacial/interglacial timescales.

[5] The Sr and Nd isotopic composition of deep seawater is faithfully recorded by authigenic chemical precipitates in the oceans, such as the calcite of planktonic foraminifera [*Elderfield et al.*, 1981; *Palmer*, 1985; *Vance and Burton*, 1999; *Burton and Vance*, 2000; *Vance et al.*, 2004], diagenetic Fe-Mn foraminifera coatings [*Palmer and Elderfield*, 1985; *Rutberg et al.*, 2000; *Bayon et al.*, 2002; *Vance et al.*, 2004] or hydrogenous Fe-Mn crusts [*Abouchami and Goldstein*, 1995; *Abouchami et al.*, 1997, 1999; *Godfrey et al.*, 1997; *Albarède et al.*, 1998; *Reynolds et al.*, 1999; *van de Flierdt et al.*, 2002, 2004a; *Piotrowski et al.*, 2004]. The conservative behavior of Sr and its marine residence time of several Myr, mean that the $^{87}Sr/^{86}Sr$ ratio of authigenic precipitates is uniform over glacial-interglacial timescales at 0.70916, i.e., the modern value of seawater [e.g., *Veizer et al.*, 1999]. However, Nd is depleted in the surface open ocean, and it is characterized by a relatively short residence time (<1 kyr [*Tachikawa et al.* [1999]). Hence the $^{143}Nd/^{144}Nd$ ratios as expressed in ε_{Nd} values, can be used to trace changes in the contribution of seawater masses and the extent of interaction at the ocean-margin interface, for example [*Patchett et al.*, 1984; *White et al.*, 1986; *Albarède et al.*, 1998; *Piotrowski et al.*, 2000; *van de Flierdt et al.*, 2002; *Lacan and Jeandel*, 2001, 2005a]. For example, *Burton and Vance* [2000] and *Vance and Burton* [1999] used foraminiferal calcite from marine sediment to reconstruct the surface water Nd isotope composition in the Labrador Sea for the past 2.5 Myr and in the Bay of Bengal for the past 150 kyr. In the latter case, they interpreted the variation in Nd isotope composition in terms of changes in riverine Nd inputs as a function of monsoonal circulation. However, there are large uncertainties in the true Nd content of foraminiferal calcite prior to formation of Fe-Mn oxyhydroxides coatings in the sediment [*Pomies et al.*, 2002]. In another study, *van de Flierdt et al.* [2004b] showed that Antarctic Bottom Water is advected northward and mixed with overlying Pacific deep water using the Nd and Hf isotopic compositions of Pacific Ocean ferromanganese nodules covering the past 38 Myr. However, the use of Nd isotopes to address short-timescale variations is hindered by the slow growth rate of Fe-Mn crusts (10^5–10^6 year per mm).

[6] Recently, *Rutberg et al.* [2000], *Bayon et al.* [2002] and *Piotrowski et al.* [2004] showed that the Fe-Mn oxide components of deep-sea cores and carbonate foraminifera can be used to trace Nd isotopic variability in the oceans on glacial-interglacial timescales. A study of the Nd isotopic compositions of the Fe-Mn oxide component from two sediment core in the southeast Atlantic suggested that the export of North Atlantic Deep Water (NADW) to the Southern Ocean was reduced during glacial stages, but was similar to the modern value during interglacial intervals throughout the past 67 kyr [*Rutberg et al.*, 2000]. However, *Bayon et al.* [2004] pointed out that such studies could encounter serious complications due to the occurrence of ''preformed'' Fe-Mn oxyhydroxide detrital material in deep-sea cores, which may mask the true seawater Nd isotopic compositions. Partial dissolution of aeolian dust in the water column releases a Fe-Mn component, which contributes to the precipitation of authigenic Fe-Mn oxyhydroxides. Such authigenic precipitates carry a detrital-terrestrial Nd signature, which is very different from that of seawater. As a consequence, the Nd isotopic composition of the Fe-Mn oxides within deep-sea sediments may represent a mixture derived from seawater and dust sources instead of a pure Nd seawater signal.

[7] At mid-ocean ridges, hydrothermal vent fields produce hydrothermal particles during vigorous and turbulent mixing of hot hydrothermal fluids with cold surrounding seawater. Sulfides, sulfates and other heavy minerals deposit near the vent source [*Dymond and Roth*, 1988; *Khripounoff and Alberic*, 1991] while Fe-Mn oxyhydroxide particles, enriched in elements from seawater, are transported several kilometers away from the vent chimney by bottom currents [*Lilley et al.*, 1995; *German and Von Damm*, 2003]. *Olivarez and Owen* [1989] and *German et al.* [1990] demonstrated that precipitation of Fe-Mn oxyhydroxides acts as a net removal mechanism for REE from seawater, following initial coprecipitation of both vent and seawater derived REE with the newly formed particles. As far-field metalliferous sediments contain seawater-like REE patterns and much higher REE/Fe ratios when compared to hydrothermal particles [*Ruhlin and Owen*, 1986; *Owen and Olivarez*, 1988; *Olivarez and Owen*, 1989], it is apparent that the Fe-Mn oxyhydroxide fraction within sediment cores must scavenge/uptake REE from seawater continuously, even after deposition, until their burial [*Olivarez and Owen*, 1989; *German et al.*, 1990]. In this paper, we test the hypothesis that hydrothermal Fe-Mn oxyhydroxide particles within hydrothermal sediment cores record changes in the Nd isotopic seawater signal through time.

3. Geological Setting and Samples

[8] An important geological requirement for our study is to choose a hydrothermal vent site where the aeolian input to the hydrothermal sediment is limited. As such, the Rainbow vent site represents a good location. The Rainbow vent site is located in the rift valley of the Mid-Atlantic Ridge (MAR) at 2300 m water depth, sited on the western flank of a nonvolcanic ridge (36°14′N, 33°54′E). It lies beneath the Azores-Bermuda high-pressure system and is at the northernmost edge of the summer east-west transport path for Sahara dust [*Arimoto et al.*, 1995; *Kuss and*

Table 1. Geochemical Composition of Leach and Residue Fraction in Sediment Cores 316 and 343[a]

Sample	Mass Proportion, %	Age by ^{14}C yr	Fe%	Ca%	$CaCO_3$%	Mn	Th	U	P	V	Co	Ni	Cu	Zn	Mo	As
Sediment Core 343																
343 1–2 cm	85.35		1.86	37.95	90.12	601	0.39	0.47	917	86	19	18	440	38	1.6	34
343 4–5 cm	81.18		1.95	38.38	91.14	666	0.45	0.45	949	88	19	19	469	38	1.4	34
343 11–12 cm	90.11	5068	1.92	37.46	88.96	633	0.51	0.41	905	84	19	23	443	39	1.3	33
343 12–13 cm	88.08	5389	1.97	37.26	88.49	682	0.48	0.48	893	84	21	40	451	39	1.4	31
343 13–14 cm	89	5709	1.94	37.51	89.09	668	0.47	0.41	892	84	20	27	447	38	1.7	36
343 18–19 cm	81.87	7312	2.02	37.83	89.84	723	0.68	0.46	906	84	22	36	460	41	1.3	36
343 19–20 cm	86.86	7632	2.11	34.96	83.03	753	0.57	0.42	854	73	24	95	409	43	1.3	32
343 20–21 cm	85.95	7953	2.11	34.42	81.75	737	0.74	0.39	767	64	23	128	347	39	1.2	26
343 21–22 cm	84.97	8854	1.97	34.71	82.45	781	0.76	0.36	732	57	23	126	308	39	1.3	23
343 22–23 cm	82.8	9754	1.72	37.53	89.14	742	0.65	0.38	658	51	21	89	281	37	1.6	19
343 23–24 cm	87.43	10655	1.54	37.09	88.09	723	0.74	0.33	667	44	20	69	241	36	1.5	19
343 25–26 cm	87.59	12457	1.32	37.21	88.38	756	0.87	0.29	532	34	19	71	181	32	1.5	12
343 26–27 cm	85.26	13358	1.54	36.18	85.92	838	0.74	0.3	513	34	20	115	179	35	1.6	13
343 27–28 cm	81.78	14259	1.54	36.26	86.11	947	0.81	0.3	551	35	21	114	181	37	1.7	14
Sediment Core 316																
316 0–1 cm	84.35		2.06	41.26		811	0.46	0.41	1327	91	27	29	454	60	5.3	22
316 2–3 cm	83.8		1.97	39.56	93.96	783	0.52	0.39	1107	87	27	30	450	52	5.2	28
316 6–7 cm	86.65	4978	2.04	40.58	96.37	855	0.49	0.5	1060	91	30	27	465	55	3.6	41
316 12–13 cm	84.55	7184	1.98	40.48	96.14	851	0.63	0.41	1048	80	29	32	437	51	4.6	37
316 16–17 cm	83.6	8654	1.88	39.50	93.82	846	0.73	0.38	860	69	26	39	398	49	3.2	28
316 18–19 cm	87.07	9389	1.76	37.98	90.19	802	0.73	0.41	830	68	26	30	380	46	3.8	32
316 20–21 cm	83.65	10125	1.82	39.90	94.75	834	0.79	0.38	834	72	27	36	376	49	4.6	35
316 22–23 cm	80.76	10860	1.79	41.07	97.55	797	0.89	0.42	811	67	25	41	357	50	4.0	30
316 25–26 cm	76.45	11963	1.47	42.40		834	0.91	0.3	526	38	25	55	221	53	4.0	18
316 26–27 cm	80.32	12331	1.26	40.30	95.72	790	0.91	0.32	670	31	25	66	194	52	3.0	3

[a]The ^{14}C ages are from *Cave et al.* [2002]. Fe%, and Ca% contents are from *Chavagnac et al.* [2005]. Ca% were corrected by a 5% error on content determination (error by ICP-AES analysis). $CaCO_3$% are calculated according to $CaCO_3\% = 2.5 * Ca\%$. All trace elements are in ppm.

Kremling, 1999; *Watkins and Maher*, 2003]. Only sediment cores along the MAR between 5°N and 35°N contain a substantial North African dust component [*Balsam et al.*, 1995]. Aeolian input of detrital clay to the sediment core at Rainbow is limited to ~1 mg/m^2/day [*Kuss and Kremling*, 1999; *Chavagnac et al.*, 2005], compared to the overall sediment accumulation rate of ~50 mg/m^2/day [*Cave*, 2002] (Table 1).

[9] The Rainbow hydrothermal vent is distinct from most hydrothermal vent sites on the MAR in that it is hosted in serpentinized peridotites, exposed at the intersection between the nontransform fault system and ridge faults in a second-order ridge discontinuity [*German et al.*, 1996]. Topographically controlled flow forces the neutrally buoyant plume to disperse north and then east away from the Rainbow site, following around the flanks of the nonvolcanic Ridge in a clockwise fashion into the adjacent section of the rift valley [*German et al.*, 1998; *Thurnherr and Richards*, 2001; *Thurnherr et al.*, 2002].

[10] The Rainbow site is composed of at least 10 groups of black smokers that expel ~360°C vent fluids characterized by high chlorinity (750 mM), low pH (~2.8), very high Fe concentrations (24 mM) and high gas concentrations [*Holm and Charlou*, 2001; *Charlou et al.*, 2002; *Douville et al.*, 2002]. The unusually high concentrations of methane and dissolved H_2 concentrations compared to basaltic systems result from Fischer-Tropsch-type synthesis in which magmatic and/or seawater-derived CO_2 is reduced to methane [*Holm and Charlou*, 2001; *Seyfried et al.*, 2004]. The chimneys and massive sulfides, which are built on ultramafic rocks and dispersed over the entire field, are enriched in Cu, Zn, Co and Ni compared with other sites in basaltic environments [*Fouquet et al.*, 1997; *Marques et al.*, 2006]. Precipitation of dissolved Fe within the overlying plume produces particle enrichments at least as high as those observed above the TAG vent field (26°N, MAR) [*German et al.*, 1996; *Edmonds and German*, 2004], such that the hydrothermal plume can be detected 50 km away from the vent site using optical backscatter [*German et al.*, 1996, 1998].

[11] During PF Poseidon cruise 240, in 1998, two box cores (core 343 taken 2 km "down-plume" at 2540 m depth and core 316 at 5 km "down-plume" at 2322 m depth) were collected downstream of the vent field, directly under the trajectory of the dispersing nonbuoyant plume. The sediments make up mainly pale brown carbonate oozes ($CaCO_3$ = 78.5–86.2%), with <5% terrigenous aluminosilicate material and low organic carbon concentrations (<0.25%). The remainder of the core is largely composed of hydrothermal oxyhydroxides, with lesser amounts of hydrothermal sulfate and sulfides [*Cave et al.*, 2002; *Chavagnac et al.*, 2005]. The ^{210}Pb and ^{14}C analyses established that the two sediment cores accumulated at 2.72 and 3.12 cm/kyr, with a well-developed surface mixed layer (top 5 cm of sediment core). The age of the surface mixed layer varies from 3.1 to 4.6 kyr [*Cave et al.*, 2002]. The deepest portion of both sediment cores is at least 12–14 kyrs old.

4. Analytical Methods

4.1. Sample Dissolution

[12] Both sediment cores were sliced at 1 cm intervals, weighed, dried and powdered in an agate mortar to minimize

trace metal contamination during sample preparation [*Cave*, 2002]. The 250–300 mg of bulk sediment from each interval was dissolved in a two-step dissolution procedure. A solution of 6M HCl was added to the sample at room temperature for less than 30 min to allow total dissolution of the biogenic carbonate and hydrothermal oxyhydroxides. The resultant solution, termed the "leach" fraction, was centrifuged and separated from the residue. The residue was rinsed three times with ultrapure water. The residue was then taken to dryness on a hotplate, and reweighed, thereby allowing the leach and residue proportions within the bulk sediment to be determined. Following weighing, these residues were then completely dissolved on a hot plate (~130°C) using a 3:1 mixture of concentrated HF and HNO_3.

[13] The use of high-molarity HCl, with or without HF, has been widely employed to dissolve Fe-Mn nodules [e.g., *Piepgras et al.*, 1979; *Abouchami et al.*, 1997, 1999; *Ling et al.*, 1997; *Vlastélic et al.*, 2001; *van de Flierdt et al.*, 2002, 2004a, 2004b]. In our technique, we did not add HF to 6 M HCl of the leach solution, so as to avoid any dissolution of silicate-bearing material, which would have overprinted the seawater signature recorded by biogenic carbonate and Fe-Mn oxyhydroxides. The average Bostrom index (100*Al/Al + Fe + Mn) of the leach fraction (mean = 20, n = 24) is considerably lower than that of the residue fraction (mean = 60, n = 24). Indeed, pelagic sediment cores, which are composed only of biogenic carbonate and detrital material, exhibit index values superior to 50 [*Cave et al.*, 2002]. Although Fe and Mn are considerably enriched in hydrothermal particles relative to Al, the Bostrom index also reflects the fact that significant levels of dissolved Al are also scavenged from Atlantic bottom waters by hydrothermal particles [*Lunel et al.*, 1990]. Overall, the data indicates that the leach fraction is not significantly impacted by lithogenic overprinting [*Chavagnac et al.*, 2005].

4.2. Geochemical Analyses

[14] Geochemical measurements were performed on a single aliquot of the dissolved sample. Trace element concentrations (P, V, Co, Ni, Cu, Zn, Mo, As) in the leach and residual solutions were determined by ICP-AES analyses using a Perkin Elmer Optima 4300 DV instrument at the National Oceanography Centre, Southampton (NOCS). The ICP-AES was calibrated using matrix-matched synthetic standards and routinely achieved a precision of 3–5% or better. Other trace elements (e.g., Th and U) were analyzed by ICP-MS using a VG PQ2+ instrument. The REE data were previously published by *Chavagnac et al.* [2005]. The ICP-MS was calibrated against a series of international rock standards, which were run before, during and after each group of analyses. Drift correction was performed by repeat analysis (every 5 samples) of a "drift monitor" standard spiked with a 10 ppb In-Re solution (internal reference). Precision and accuracy in these analyses were routinely better than 3% [see *Chavagnac et al.*, 2005]. The reagents used in the leaching and dissolution procedures are all high-purity, double subboiled distilled acids. Hence the blanks for all elements considered here are $\ll$1% of the analyte.

4.3. Sr and Nd Isotope Measurements

[15] For Nd isotopic analyses, Nd was separated from the matrix using a routine two column ion exchange technique, including first, a group of REE through a cation exchange column, followed by isolation of Nd through a second column packed with Kel-F Teflon coated hydrogen di-ethylhexyl phosphate (HDEHP). Sr was isolated using Sr-Spec resin (Eichrom, USA). Sr and Nd isotope ratios were measured at NOCS on a VG Sector 54 mass spectrometer. The $^{87}Sr/^{86}Sr$ and $^{143}Nd/^{144}Nd$ ratios were determined as the average of 150 ratios by measuring ion intensities in multi-dynamic collection mode. The $^{87}Sr/^{86}Sr$ and $^{143}Nd/^{144}Nd$ ratios were normalized to $^{86}Sr/^{88}Sr = 0.1194$ and $^{146}Nd/^{144}Nd = 0.7219$, respectively. Measured values for NBS 987 and JNd-i standards (recommended values of 0.710250 and 0.512100, respectively) were $^{87}Sr/^{86}Sr = 0.710244 \pm 24$ (2σ, n = 56) and $^{143}Nd/^{144}Nd = 0.512104 \pm 10$ (2σ, n = 38), respectively.

5. Results and Discussion

[16] Biogenic carbonate contains very low concentrations of REE (<0.3 ppm Nd [*Palmer*, 1985]), hence the Nd isotope composition of the leach fraction is dominated by that of the oxyhydroxide component. The REE concentration of oxyhydroxides in hydrothermal particles at Rainbow reflects a mixture of REE derived from seawater and hydrothermal fluids [*Edmonds and German*, 2004]. The ε_{Nd} values of end-member hydrothermal fluids are similar to submarine basalt (i.e., ~+10), which is much higher than the ε_{Nd} values of Atlantic seawater (i.e., ~−9 to −15) [*Piepgras and Wasserburg*, 1987]. In addition, the Nd concentration of Rainbow hydrothermal fluids is ~800 times higher than that of local seawater [*Douville et al.*, 2002]. Hence, if the oxyhydroxide component of hydrothermal sediments is to provide an accurate record of seawater ε_{Nd} values, the contribution of Nd from hydrothermal fluids to the oxyhydroxides must be minimal.

[17] We argue in the following paragraphs that the geochemical and isotopic composition of the leach fraction is dominated by that of seawater rather than hydrothermal inputs, based on the transition metal distributions, REE patterns and Sr isotope data.

5.1. Transition Metal Contents of the Leach Fraction

[18] Major and trace element composition of the leach fraction on both sediment cores are reported as raw data in Table 1. To correct for carbonate dilution (carbonate contains very low levels of trace elements), we calculated major and trace element contents on a carbonate free basis (cfb) using the following equation: $[El]_{cfb} = 100 * [El]_{leach}/(100 - [CaCO_3\%])$ [e.g., *Schaller et al.*, 2000]. This step is necessary to more closely examine the hydrothermal input to the leach fraction as the bulk sediment core is composed of >79% of biogenic carbonate.

[19] Fresh Fe and Mn oxyhydroxide phases are precipitated from hydrothermal plumes via chemical reactions during the progressive, rapid mixing of hydrothermal fluid with seawater. These phases are chemically active and scavenge dissolved trace metals from the water column [*Edmond et al.*, 1982]. Hence hydrothermal particles col-

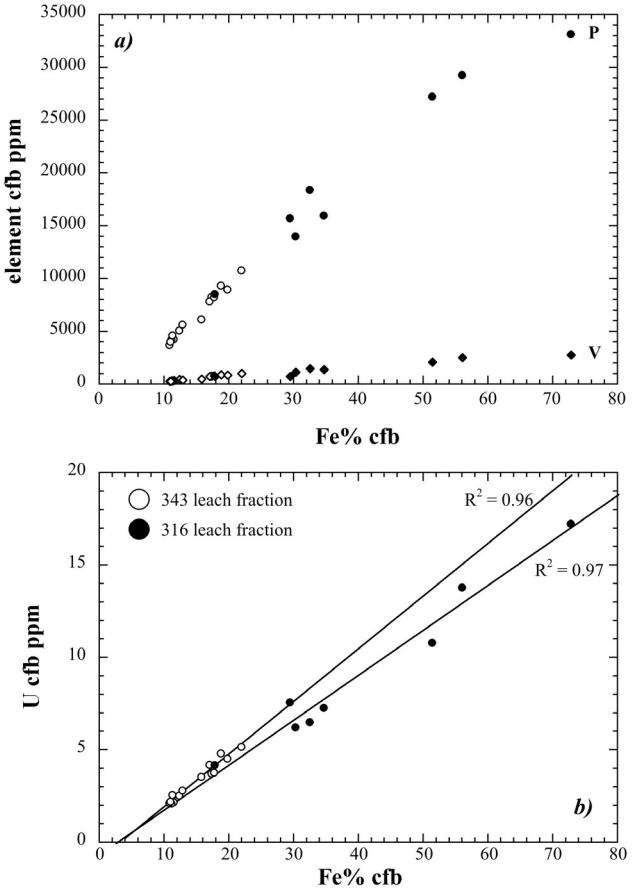

Figure 1. P_{cfb}, V_{cfb}, and U_{cfb} contents as a function of Fe_{cfb}% for 316 and 343 leach fractions. (a) Element cfb. Circles represent P_{cfb}; diamonds represents V_{cfb}. (b) U_{cfb}. Open symbols represent core 343; solid symbols represent core 316. Circles represent P; diamonds represent V.

lected from neutrally buoyant plumes exhibit a positive linear relationship between Fe and oxyanion-forming metal concentrations [*Trefry and Metz*, 1989; *Feely et al.*, 1990, 1992, 1994; *German et al.*, 1991; *Metz and Trefry*, 1993; *Ludford et al.*, 1996]. Figure 1 plots the P_{cfb}, V_{cfb} and U_{cfb} contents as a function of Fe_{cfb}% for both leach fractions. In all cases, we observe a positive linear relationship ($r^2 > 0.93$) with an intercept close to zero. The P, V and U contents observed in the leach fraction cannot be explained solely by a hydrothermal source as newly formed hydrothermal particles contain very low amounts of P, V and U (1 to 60 nmol/L, 40 to 2100 nmol/L and 0.020 pmol/L, respectively) [*Edmonds and German*, 2004]. Clearly, additional uptake is required, providing strong evidence that the oxyanion source of the leach fraction is dominated by seawater-derived uptake rather than by hydrothermal input. The hydrothermal input is best seen by the high Fe concentrations and positive linear correlations between transition metals and Fe (Figure 2). The Zn, Cu and Co contents of Fe oxyhydroxide particles (Zn = 0.05–3.3 nmol/L; Cu = 0.03–7.7 nmol/L; Co = 1.8–173 pmol/L [*Edmonds and German*, 2004]) are of the same order of magnitude as seawater values (Zn ≈ 6 nmol/L; Cu ≈ 4 nmol/L; Co = 20 pmol/L [*Millero*, 1996]). The high concentrations of transition metals (several ppm) in terrigenous aluminosilicates mean that the presence of significant amounts of this material would eradicate the element-element linearity seen in Figure 2 between seawater and hydrothermal endmembers. Hence the high degree of linearity of these correlations testifies to the lack of external, additional input (such as detrital matter) within the leach fraction.

[20] On the basis of the transition metals and oxyanion distribution, we argue that (1) the trace metal content of the

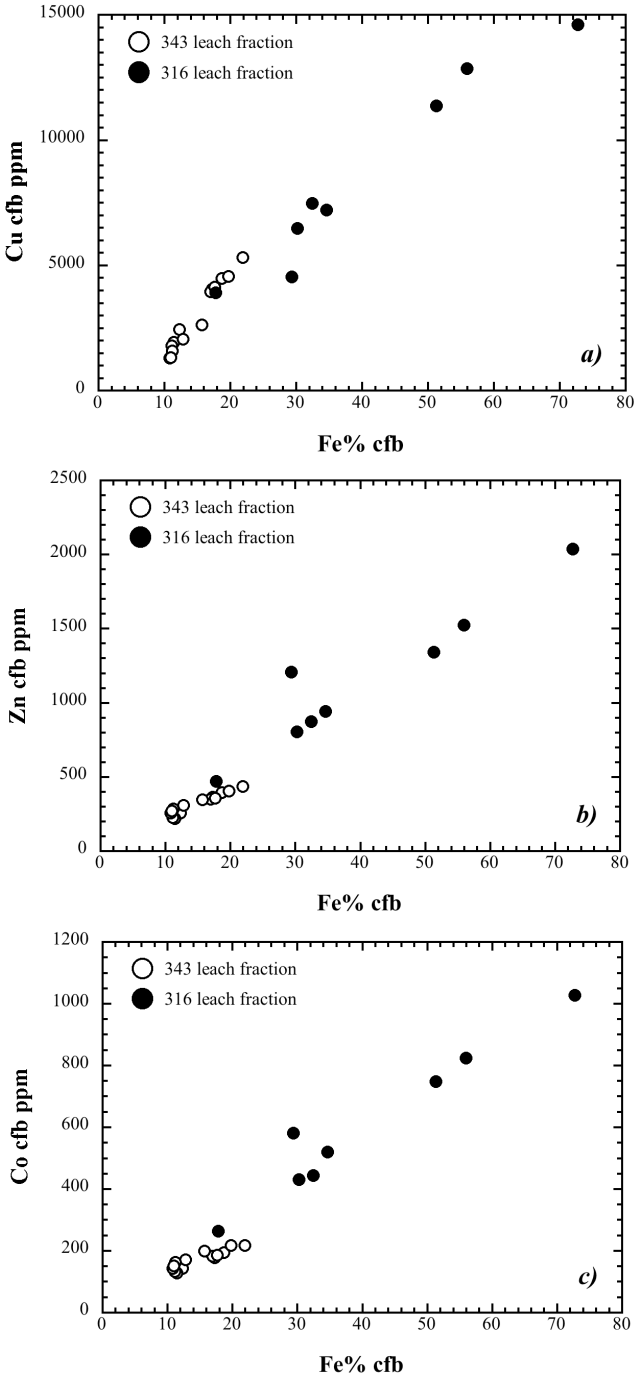

Figure 2. (a) Cu_{cfb}, (b) Zn_{cfb}, and (c) Co_{cfb} contents as a function of Fe_{cfb}% for 316 and 343 leach fractions.

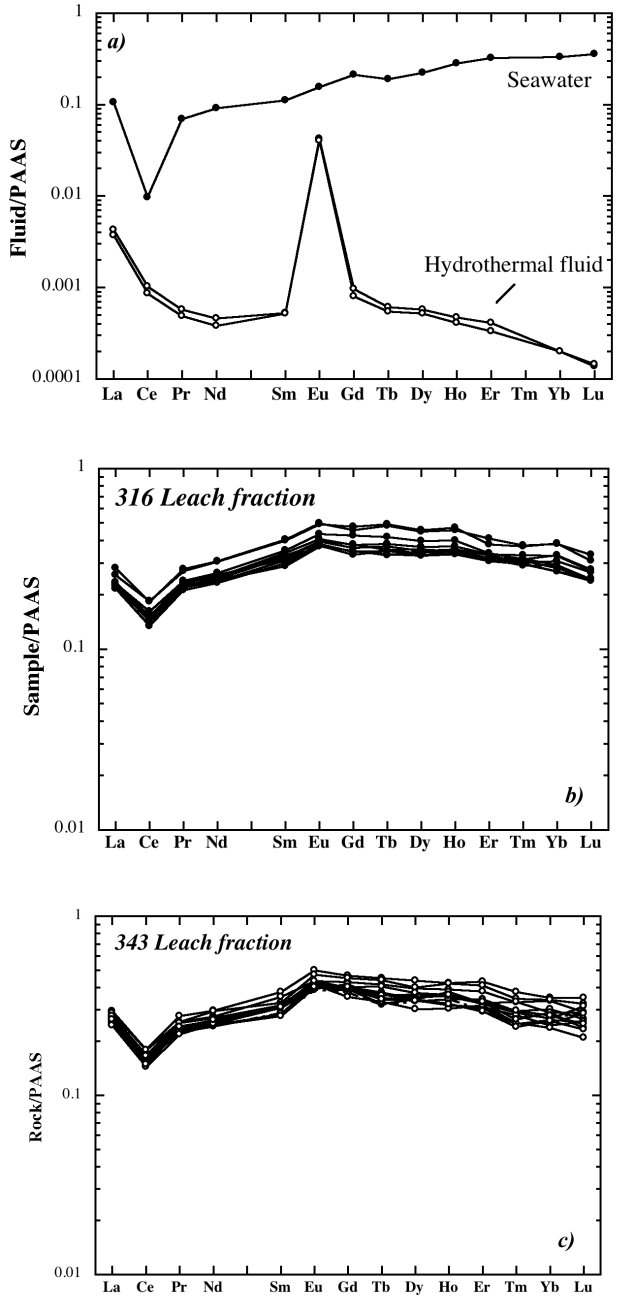

Figure 3. (a) REE patterns of hydrothermal fluids and local seawater (fluid $\times$ 10^6) from the Rainbow hydrothermal site [*Douville et al.*, 2002]. (b) REE patterns of the leach fraction of sediments from core 316. (c) REE patterns of the leach fraction of sediments from core 343. Normalization values of post-Archean average Australian sedimentary (PAAS) rock [*McLennan*, 1989] are shown.

leach fraction is controlled by those of seawater and hydrothermal input and (2) no detrital sediment contributes to the trace metal contents of the leach fraction.

5.2. REE Contents of the Leach Fraction

[21] The hydrothermal contribution to the leach fraction can be assessed using REE patterns. The REE patterns of hydrothermal fluids and seawater (multiplied by 10^6) are very distinct from one another (Figure 3). Seawater is characterized by a negative Ce anomaly and HREE (Heavy REE) enrichment because of complexation and redox chemistry processes [*Turner and Whitfield*, 1979]. The anomalously low dissolved Ce content of seawater is due to its oxidative removal as highly insoluble $Ce(IV)O_2$. In contrast, hydrothermal fluids lack a negative Ce anomaly – Ce is trivalent in vent fluids in reducing conditions – but show a pronounced positive Eu anomaly inherited from plagioclase during fluid-rock interaction [*Sverjensky*, 1984]. Hydrothermal particles act as a net sink for the REE from seawater and can have REE patterns mimicking both seawater and hydrothermal fluid with negative Ce and positive Eu anomalies, respectively, [*German et al.*, 1990].

[22] Leach fractions from both cores show seawater and hydrothermal fluid REE features. The negative Ce anomaly indicates that the Fe-Mn oxyhydroxides within the leach fraction formed rapidly. This contrasts to hydrogenous Fe-Mn phases, which grow slowly and contain a positive Ce anomaly. The relative contributions of REE in the leach fraction from REE from seawater and hydrothermal fluid can be calculated qualitatively from the Eu anomaly ($Eu/Eu^* = 2 * Eu_N/(Sm_N + Gd_N)$) (post-Archean average Australian sedimentary rock (PAAS) normalization values) of the leach fraction, based on the Eu/Eu* values of the hydrothermal fluid (Eu/Eu* = 57.1) and local bottom water (Eu/Eu* = 0.96) [*Douville et al.*, 2002]. This calculation reveals that the average fraction of hydrothermal REE in the leach fraction is only 0.35% of the total REE (range 0.22–0.65%). This would only perturb the ε_{Nd} value of the leach phase by a maximum of 0.13 ε_{Nd} units, assuming an end-member hydrothermal ε_{Nd} value of +10. This is smaller than the average analytical uncertainty ($\pm$ 0.2 units) in the ε_{Nd} values. The lack of a positive correlation between the ε_{Nd} values and the Eu anomalies also argues against a significant hydrothermal fluid Nd contribution to the leach (Figure 4 and Tables 1 and 2), as does the fact that the ε_{Nd} values do not correlate with transition metal or Fe

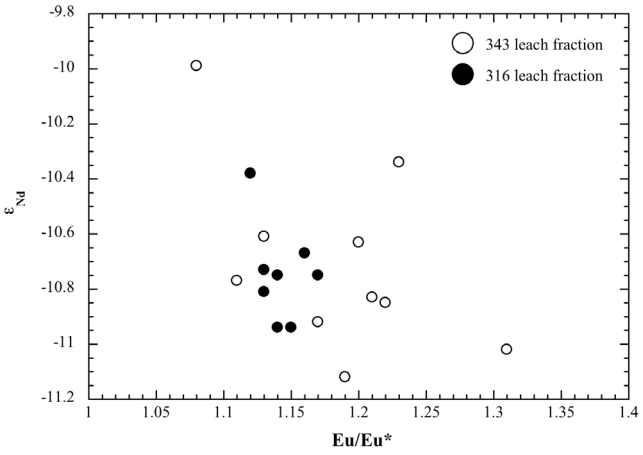

Figure 4. The $\varepsilon_{Nd}(0)$ values as a function of Eu/Eu* anomaly ($2 \times Eu_n/(Sm_n + Gd_n)$) on leach fractions from cores 343 and 316.

Table 2. Sr and Nd Isotope Data on the Leach and Residue Fraction in Sediment Cores 316 and 343[a]

Sample	Mass Proportion, %	Age by ^{14}C Year	Eu/Eu*	Fe%	Sr, ppm	$^{87}Sr/^{86}Sr$	± 2 SE	Nd, ppm	143Nd/144Nd	± 2 SE	eNd(0)	± 2 SE
Sediment Core 343												
343 1–2 cm	85.35		1.05	1.86	1615	0.709183	0.000008	10.09	ND	ND	ND	ND
343 4–5 cm	81.18		0.98	1.95	1708	0.709171	0.000009	9.33	ND	ND	ND	ND
duplicate						0.709171	0.000009					
343 11–12 cm	90.11	5068	1.09	1.92	1608	0.709161	0.000008	8.42	0.512108	0.000005	−10.34	0.10
343 12–13 cm	88.08	5389	1.07	1.97	1514	0.709184	0.000010	10.01	0.512083	0.000012	−10.83	0.23
343 13–14 cm	89.00	5709	1.04	1.94	1589	0.709166	0.000008	8.84	0.512162	0.000005	−9.29	0.10
343 18–19 cm	81.87	7312	0.99	2.02	1638	0.709173	0.000009	8.62	0.512086	0.000006	−10.77	0.12
343 19–20 cm	86.86	7632	1.03	2.11	1503	0.709176	0.000007	8.29	0.512078	0.000005	−10.92	0.10
343 20–21 cm	85.95	7953	0.96	2.11	1461	0.709165	0.000008	8.49	0.512126	0.000006	−9.99	0.12
duplicate						0.709150	0.000009					
343 21–22 cm	84.97	8854	1.08	1.97	1410	0.709128	0.000009	8.24	0.512082	0.000006	−10.85	0.12
343 22–23 cm	82.80	9754	1.06	1.72	1528	0.709147	0.000007	8.89	0.512093	0.000006	−10.63	0.12
duplicate						0.709127	0.000009					
343 23–24 cm	87.43	10655	1.16	1.54	1374	0.709140	0.000007	8.32	0.512073	0.000006	−11.02	0.12
343 25–26 cm	87.59	12457	1.07	1.32	1382	0.709171	0.000007	9.16				
343 26–27 cm	85.26	13358	1.05	1.54	1307	0.709154	0.000009	8.49	0.512068	0.000006	−11.12	0.12
343 27–28 cm	81.78	14259	1.00	1.54	1333	0.709158	0.000007	8.92	0.512094	0.000020	−10.61	0.39
Sediment Core 316												
316 0–1 cm	84.35		1.14	2.06	1005	0.709154	0.000009	8.71	0.512091	0.000007	−10.67	0.14
316 2–3 cm	83.80		1.17	1.97	3008	0.709175	0.000008	8.13	0.512087	0.000006	−10.75	0.12
316 6–7 cm	86.65	4978	1.14	2.04	2507	0.709161	0.000007	7.91	0.512087	0.000006	−10.75	0.12
316 12–13 cm	84.55	7184	1.13	1.98	2487	0.709152	0.000007	8.26	0.512088	0.000006	−10.73	0.12
316 16–17 cm	83.60	8654	1.16	1.88	2428	0.709169	0.000007	8.06	0.512091	0.000006	−10.67	0.12
316 18–19 cm	87.07	9389	1.14	1.76	2755	0.709180	0.000006	8.29	0.512077	0.000006	−10.94	0.12
316 20–21 cm	83.65	10125	1.13	1.82	1759	0.709164	0.000007	8.50	0.512084	0.000006	−10.81	0.12
316 22–23 cm	80.76	10860	1.15	1.79	2350	0.709153	0.000007	10.37	0.512077	0.000006	−10.94	0.12
316 25–26 cm	76.45	11963	1.11	1.47	3925	0.709167	0.000006	8.97	0.512098	0.000010	−10.53	0.20
316 26–27 cm	80.32	12331	1.12	1.26	5020	0.709165	0.000006	10.34	0.512106	0.000006	−10.38	0.12

[a]ND is not determined.

concentrations (not shown). In addition, the Ce anomalies ($Ce/Ce^* = 3*Ce_N/(2*La_N + Nd_N)$ and Nd/Yb_N) ratios clearly indicate that the Fe-Mn oxyhydroxides within the leach fraction have a seawater origin ($Ce/Ce^* \sim 0.1$) because hydrogenous Fe-Mn oxides have strong positive Ce/Ce* values [*Mills et al.*, 2001].

[23] The amount of REE originating from hydrothermal source present within the leach can be estimated from the Fe and Nd contents. Unaltered biogenic carbonate contains very low levels of Fe and Nd [*Palmer*, 1985], suggesting that Fe and Nd contents of the leach fraction is fully of hydrothermal origin. However, hydrothermal particles collected from the water column at sites 343 and 316 have average Nd/Fe ratio of 0.4 and 3.4×10^{-4}, respectively [*Edmonds and German*, 2004], which are lower than those of the leach fraction Nd/Fe ratios of $3.9–8.2 \times 10^{-4}$. This suggests that the leach Nd budget is not solely accounted for by hydrothermal input. Because Fe-Mn oxyhydroxides within the buoyant plume initially scavenge and then take up REE from seawater [*Owen and Olivarez*, 1988; *Olivarez and Owen*, 1989; *German et al.*, 1990; *Edmonds and German*, 2004], we propose that the vast majority (>99%) of the REE present within the leach fraction is of seawater origin.

5.3. Potential Modification of the Seawater Nd Isotope Signature

[24] It is important to discuss the potential processes such as diagenesis, pore water overprinting, and seawater-hydrothermal particle interactions, which could lead to REE fractionation and modification of the Nd seawater signature record in the leach fraction. We will also discuss whether the Nd hydrothermal input can modify the Nd isotope signature of the local seawater mass and when the hydrothermal particle acquires their Nd isotope signature.

[25] We define fractionation here as a relative change in the REE particle composition due to geochemical reactions. REE have been measured previously in neutrally buoyant and buoyant plume particles at Rainbow hydrothermal site [*Edmonds and German*, 2004; *Douville et al.*, 2002]. The REE concentrations of Fe-Mn oxyhydroxide particles display a positive curvature with respect to particulate Fe [*German et al.*, 1990], which is attributed to continuous uptake of REE from seawater onto hydrothermal particles as the plume disperses, following an initial coprecipitation of both hydrothermal and seawater derived REE. *Edmonds and German* [2004] demonstrated that high REE/Fe ratios of hydrothermal sediments compared to hydrothermal particles is evidence of continuous uptake of REE from seawater [see also *Ruhlin and Owen*, 1986]. In addition, *Sherrell et al.* [1999] argued that the REE patterns of particles from East Pacific Rise hydrothermal sites reflect those of local seawater. Both studies provide ample evidence that the hydrothermal particles contain Nd derived from ambient seawater and would thus be expected to record the Nd isotopic composition of this seawater at the time of their deposition at the sediment-water interface.

[26] On the basis of the following arguments, we do not believe that postdepositional diagenesis has affected the

REE distributions within the two sediment cores considered here. Mn enrichments in near-surface sediments are common in the deep-sea environment because of the reduction of Mn oxides at depth and the upward diffusion of Mn^{2+}, leading to the formation of Mn oxyhydroxides in oxic conditions close to the sediment surface. A reducing environment can be established within the sediment when the sediment accumulation rate is high enough to bury organic matter before it is oxidized [*Wilson et al.*, 1985]. However, the two sediment cores considered here are accumulating at several cm kyr^{-1} under oxic bottom water conditions and contain very low amounts of organic carbon (<0.46% [*Cave et al.*, 2002]), and therefore do not favor development of a suboxic environment. In addition, if the redox conditions within the sample had changed significantly then, redox sensitive elements such as U and Mn [*Klinkhammer and Palmer*, 1991] would show clear breaks in their concentration-depth profiles marking the depth of the redox front. The lack of such relationships for Mn and U and the constant Ce/Ce* anomalies through the cores (typical of seawater like signature) strongly indicate that the redox conditions remained suboxic in the upper ~40 cm of these sediments. Hence the elevated Mn levels seen in these sediment cores are most likely of a hydrothermal rather than diagenetic origin.

[27] From a recent study of the REE distribution in pore water of marine sediments from anoxic to oxic conditions, *Haley et al.* [2004] showed that remineralization of organic coatings is the primary REE source in oxic pore water [see also *Goldberg et al.*, 1963; *Elderfield and Greaves*, 1982; *Sholkovitz*, 1992]. Such pore waters exhibit "linear" type REE patterns, which would drastically modify the REE pattern of the leach fraction if Fe-oxide had interacted with the pore water. However, the REE patterns of the Fe-Mn oxyhydroxide particles of the leach fraction exhibit MREE enrichment ("bulge pattern") associated with negative Ce anomalies. Such patterns are typical of Fe oxide scavenging REE from seawater.

[28] Hydrothermal vent fluids have Nd concentrations more than 500 times greater than seawater, and may potentially change the Nd isotope signature of seawater. A contribution of 0.02% of hydrothermal fluid will be needed to modify the Nd isotope signature of seawater by more than 1 ε_{Nd} unit at the orifice of the vent chimney. However, the buoyant plume will be diluted, in an hour, to 10 000:1 after less than 1 km covered [*German and Von Damm*, 2003], suggesting that the Nd hydrothermal input to seawater is negligible. Moreover, the Nd isotopic composition is uniform in metalliferous sediments at distances within 10 km of the ridge because hydrothermal Nd is quickly scavenged by hydrothermal particulates [*Halliday et al.*, 1992]. These data indicate that hydrothermal vent fluids have no effect on Nd isotopic composition of seawater [*Halliday et al.*, 1992].

[29] Finally, *Olivarez and Owen* [1989], *Owen and Olivarez* [1988], and *German et al.* [1990] showed that hydrothermal particles initially scavenge REE from the hydrothermal plume and then take up REE from seawater. Leach fractions have Nd/Fe ratios of $3.9-8.2 \times 10^{-4}$, which exceed those of hydrothermal particles ($0.4-3.4 \times 10^{-4}$) collected from the water column at the site of the sediment cores [*Edmonds and German*, 2004]. Hence the Nd budget of the leach fraction is a mixture of Nd derived directly from the deep water through which the particles passed before sedimentation and Nd adsorbed after the particles settled at the seafloor. The surface mixed layer homogenizes the top 5 cm of the sediment core over a period of 100 years after deposition from the water column [*Cave et al.*, 2002] and particles within this layer are exposed to overlying seawater Nd isotope compositions and REE patterns. Once the particles are buried below this surface layer there is the potential for them to be exposed to Nd isotopes and REE released from other sedimentary components during diagenesis. However, our observations (see above) of key diagenetic indices (Ce anomalies, U concentrations, etc.) indicate that the sediments in the upper ~40 cm of these cores have not undergone the intensity of diagenesis sufficient to result in wide-scale mobilization of REE. This hypothesis is further supported by the observation (see above) that the REE patterns of the leach fractions are typical of bottom water (with the addition of positive Eu anomaly originating from hydrothermal material) and are not influenced by pore waters. Hence we believe that there is strong evidence to suggest that the Nd isotope and REE signatures of the leach fraction reflects that of the overlying seawater, and that these signatures are preserved until the sediments are buried well below the horizons sampled in this study.

5.4. Sr Isotope Data

[30] The Sr and Nd isotope data for the leach fractions of both cores are reported in Table 2. Hydrothermal Fe-Mn oxyhydroxides contain low amounts of Sr (~5–26 ppm (V. Chavagnac, unpublished data, 2003)) compared to biogenic carbonate, which contains ~1000 ppm Sr. Hence biogenic carbonate dominates the Sr isotope composition of the leach fraction, and it is no surprise that the leach fractions from cores 343 and 316 have average $^{87}Sr/^{86}Sr$ ratios of 0.709160 and 0.709164, respectively, i.e., indistinguishable from that of modern seawater at 0.709160. Given that detrital clay from a nearby hydrothermal site has an average $^{87}Sr/^{86}Sr$ ratio of 0.7229 and an average Sr concentration of ~115 ppm [*Severmann et al.*, 2004], these data indicate that <0.5% of the leach fraction is derived from dissolution of detrital material.

5.5. Interim Conclusions

[31] Although a full evaluation of the potential of hydrothermal sediments as a proxy for ε_{Nd} values would ideally include Nd isotope analyses of particles collected from the hydrothermal plume and ambient seawater, this has not proved possible thus far. In addition, this exercise is made more problematic by the low concentration of Nd of hydrothermal particles and the small amount of material that it has been possible to collect (1.2–7.8 pmol/L [*Edmonds and German*, 2004]).

[32] Despite the lack of this conclusive data, we present the following arguments to suggest that the Nd isotope composition of the leach fraction of the hydrothermal sediments considered in this study provide a record of the ε_{Nd} values of contemporaneous ambient seawater: (1) Studies of

the REE geochemistry of particles collected from non-buoyant hydrothermal plumes show that they are dominated by seawater-derived REE. (2) The overall geochemistry of the leach fraction indicates that there is no significant detrital contribution to this phase. (3) Comparison of the REE patterns of the leach fraction of the hydrothermal sediments in this study with seawater and hydrothermal fluids indicates that <0.65% of the total REE in the leach fraction are derived from a hydrothermal source. (4) The sediments have not undergone suboxic diagenesis and therefore retain their original depositional ε_{Nd} values. (5) The Sr isotope data indicate that the detrital contribution to the leach fraction is <0.5%.

5.6. Seawater Nd Isotope Signature at Present Time

[33] The present-day deepwater circulation in the Rainbow rift valley is characterized by inflow of North East Atlantic Deep Water (NEADW) from the eastern ridge flank [*Thurnherr and Richards*, 2001; *Thurnherr et al.*, 2002]. NEADW is composed of a mixture of four different water masses that mix at midlatitude in the North Atlantic and are characterized by distinct ε_{Nd} values: (1) Mediterranean Surface Water (MSW; $\varepsilon_{Nd} = -9.4$; [Nd] = 3.3 ppt), (2) Labrador Sea Water (LSW; $\varepsilon_{Nd} = -13.8$; [Nd] = 3.1 ppt), (3) Iceland-Scotland Overflow Water (ISOW; $\varepsilon_{Nd} = -8.2$; [Nd] = 3.1 ppt), and (4) Lower Deep Water (LDW; $\varepsilon_{Nd} = -13.0$; [Nd] = 3.6 ppt) [*Spivack and Wasserburg*, 1988; *Abouchami et al.*, 1999; *Van Aken*, 2000; *Lacan*, 2002].

[34] It is reasonable to compare the NEADW Nd isotope signature at our sample site to that of the Madeira Abyssal Plain (MAP) because (1) there is no topographic high between the MAR and MAP that could have modified the flow of NEADW [*Saunders*, 1982; *Sarnthein et al.*, 1994], and (2) the Rainbow rift valley is characterized by NEADW inflow from the eastern ridge flank [*Thurnherr and Richards*, 2001; *Thurnherr et al.*, 2002]. The relative contribution of the four water masses to NEADW in various basins of the northeast Atlantic during 1981–1997 was determined from conservative water properties (potential temperature, salinity, etc.) by *Van Aken* [2000]. In the MAP he calculated that the relative proportions of MSW, LSW, ISOW and LDW to NEADW were 5.2% (±1.1), 37.9% (±2.8), 14.5% (±6.8), and 42.4% (±8.4), respectively. Conservative mixing between these end-members yields a ε_{Nd} value of -12.4 ± 0.9 for NEADW at the depth of the Rainbow hydrothermal plume. Analyses of the present-day Nd isotope composition of seawater collected at 2500 m depth in the oligotrophic ocean indicate a value of -11.9 ± 0.2. This sample was taken in the immediate proximity of the MAP, which is located to the east of the section of Mid-Atlantic Ridge hosting the Rainbow site (21°N, 31°W [*Tachikawa et al.*, 1999]). The mean measured seawater Nd isotopic composition of NEADW is of -12.8 ± 0.2 [*Lacan and Jeandel*, 2005b].

[35] Additional ε_{Nd} value of the NEADW can be obtained from authigenic minerals and crusts. The present-day ε_{Nd} value of -11.9 ± 0.2 was obtained on authigenic minerals collected at the same location as the seawater sample (21°N, 31°W [*Tachikawa et al.*, 1997]), and of -12.1 to -12.3 for hydrothermal Fe-Mn crusts from TAG (26°N [*Mills et al.*, 2001]). The ε_{Nd} values of authigenic material are in agreement with the value of -11.9 ± 0.2 of seawater in the oligotrophic Atlantic, in proximity of the Rainbow vent site.

5.7. Potential Implications for Seawater Nd Isotope Signature Over the Last 14 kyr

[36] As noted above, we propose that the ε_{Nd} values recorded in the leach phase reflects the Nd isotope composition of the seawater at the time of deposition of the sediments. The ^{14}C dates from bulk carbonate within the core [*Cave et al.*, 2002] have been used to plot the Nd isotope data as a function of radiocarbon ages (Figure 5). Data from both cores are included on the same plot because (1) both sediment cores were collected within the MAR valley at similar water depth, (2) they are only located 3 km apart, and (3) NEADW is the water mass above each sediment cores. Hence the two down-core sections (Figure 5) may provide a history of seawater ε_{Nd} values at this location. Nd isotope data were limited in the top core sediment because of the well-developed surface mixed layer (top 5 cm core depth using ^{210}Pb excess), which does not allow a precise age determination based on ^{14}C ages. With the exception of four samples, the ε_{Nd} values vary within a narrow range between -10.7 and -11.1, which are all higher than the present-day NEADW ε_{Nd} value of -12.4 ± 0.9.

[37] These values are similar to those from a Fe-Mn crust (D10979) from the Madeira Abyssal Plain (5347–4867 m depth; 32°N, 24°W), which showed ε_{Nd} values between -11.1 and -10.6 over the last 7 Myr [*Reynolds et al.*, 1999] (although no ε_{Nd} values on samples younger than 196 kyr were obtained). *Abouchami et al.* [1999] report similar ε_{Nd} values of -10.8 to -11.8 over the past 10.5 Myr for a Fe-Mn hydrogenous crust (121DK) from the Tropic Seamount (2000 m depth; 24°N, 21°W). *Schmitz* [1996] reports also a similar value of -11.2 ± 0.3 for the NEADW based on the contribution of 1/3 from ISOW, 1/3 from eastern LDW and 1/3 from modified North Atlantic + LSW.

[38] Two scenarios are proposed to explain these variations: (1) changes of the ε_{Nd} value of the four source waters in the past and (2) changes in the relative contributions of the different water masses to NEADW formation. The first hypothesis is exemplified by the large variations of ε_{Nd} values of water masses that were observed during major geological event; for example, during closure of the Panama Gateway at 5 Ma [*Reynolds et al.*, 1999; *Frank et al.*, 1999]. Modification of the Nd isotope signature does not occur instantaneously, but progressively over a Myr or so. In our case, we are dealing with ε_{Nd} variations on a kyr timescale where no major geological event took place in terms of opening or closure of seawater circulation gateways, hence this scenario seems unlikely. Changes in seawater Nd isotopic composition can also occur with increasing weathering of local source rocks, aeolian and riverine inputs. However, the Rainbow vent site is located in the middle of the ocean outside the immediate reach of aeolian and riverine inputs, suggesting that the changes in ε_{Nd} values we observe are unlikely to be in response to this cause. Finally, *Lacan and Jeandel* [2001, 2005a, 2005b] demonstrated that

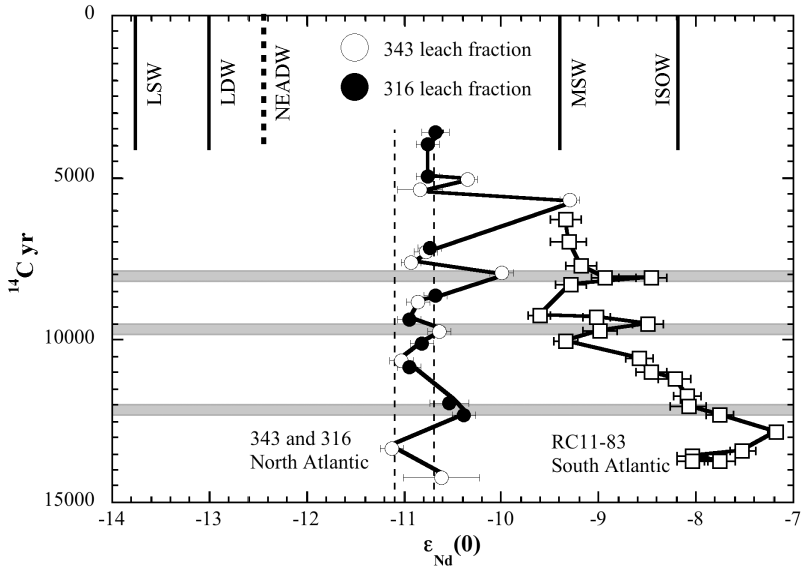

Figure 5. The ^{14}C year record of $\varepsilon_{Nd}(0)$ values in the leach phase of sediments from cores 343 and 316, compared to the $\varepsilon_{Nd}(0)$ record in the RC11-83 in the South Atlantic (data from *Piotrowski et al.* [2004]). Note that high ε_{Nd} values in the sediment core in the North Atlantic are also related to higher ε_{Nd} values in the sediment core in the South Atlantic. The variation of the ε_{Nd} values in sediment core RC11-83 is interpreted as being related to the North Atlantic Deep Water strength [*Piotrowski et al.*, 2004].

the ε_{Nd} values of seawater masses are modified when the seawater mass interacts with continental margins and oceanic slopes. However, the position of the Rainbow hydrothermal field on the MAR means that it is very unlikely that NEADW at this location was modified by interaction with the European or American margins. Hence these suggest that past variations in the ε_{Nd} values of the four source waters are the most likely cause of the higher ε_{Nd} values of seawater at the Rainbow site compared to that of the present time.

[39] Hence this suggests that variations in the ε_{Nd} values may reflect changes in the relative contributions of different water masses to NEADW formation. *Reynolds et al.* [1999] and *Abouchami et al.* [1999] suggest a strong influence of Antarctic Bottom Water (AABW), which has a ε_{Nd} value of -9 [*Jeandel*, 1993], on NADW, but the cores from Rainbow are from a depth of 2500–2300 m, which is well above the current upper limit ($\sim$4000 m) of AABW in the North Atlantic at 36°N. In addition, the Rainbow rift valley is characterized by NEADW inflow from the eastern ridge flank [*Thurnherr and Richards*, 2001; *Thurnherr et al.*, 2002]; hence it seems unlikely that AABW influences the seawater ε_{Nd} value at Rainbow. The discrepancy between the values observed from core 316 and 343 with those of NEADW, could indicate that a higher proportion of ISOW is transported southward along the Mid-Atlantic Ridge itself (reaching as far south as 30°N [*Gana and Provost*, 1993; *Van Aken and Becker*, 1996]). An increased influence of MSW seems unlikely, as it forms the top 800 m of the water that makes up the NEADW.

[40] The records from core 316 and 343 do not extend to younger ages than $\sim$4 kyr, hence an alternative reason why these sediments record less radiogenic ε_{Nd} values (-10.6 to -11.1) than current NEADW (-12.4 ± 0.9) is that the relative proportions of the four water masses that make up NEADW have changed over time. For example, temperature, salinity and density measurements indicate that the present-day contributions of these water masses to NEADW are MSW (5.2 ± 1.1%), LSW (37.9 ± 2.8%), ISOW (14.5 ± 6.8%) and LDW (42.4 ± 8.4%) [*Van Aken*, 2000]. Hence the ε_{Nd} values of our samples would appear to require an increase in the ISOW proportion to NEADW, with concomitant decreases in the contributions of LSW and LDW.

[41] At Rainbow vent site, the variation of the ε_{Nd} values vary in a narrow range between -11.1 and -10.7 apart from 4 excursions toward higher ε_{Nd} values at about 5 kyr, 8 kyr, and 12 kyr. In comparison, the variation of ε_{Nd} values on Fe-Mn oxyhydroxides from core in the South Atlantic exhibit similar excursions toward higher ε_{Nd} values at the same time interval (apart from 5 kyr where no data are available) (Figure 5) [*Piotrowski et al.*, 2004, 2005]. *Piotrowski et al.* [2004] indicate that rapid meltwater discharges to the NADW would modify the ε_{Nd} record in Fe-Mn oxy-hydroxide by one to two ε_{Nd} units, but are extremely short-lived. These authors show that sea ice coverage in the North Atlantic is correlated to changes in NADW production on a millennial scale during the deglaciation. It is tempting to speculate that at Rainbow vent site, the change of ε_{Nd} values in the leach fraction could record a change in the deep water mass as observed in the South Atlantic.

6. Conclusions

[42] Fe oxyhydroxide hydrothermal sediments are common along the length of the world's mid-ocean ridge system. Although these sediments compose a mixture of

Nd derived from hydrothermal, lithogenic and seawater sources, we have shown that it is possible to use a selective sequential leaching procedure to isolate the fraction of Nd derived from seawater and hence provide a record of deep seawater ε_{Nd} values. This leach fraction is a mixture of biogenic carbonate and hydrothermal Fe-Mn oxyhydroxide, and its oxyanion and REE contents are most likely of seawater origin.

[43] A preliminary test of this technique suggest that, in the vicinity of the Rainbow hydrothermal site, Iceland-Scotland Overflow Water formed a higher contribution to the North East Atlantic Deep Water between 4 and 12 ka that is observed at present time. As a corollary, the data also suggest that the relative contributions of Labrador Sea Water and Lower Deep Water to the Madeira Abyssal Plain of NEADW were smaller during 4–12 ka than they are today.

[44] Although further studies are required to distinguish between these hypotheses, we believe the ε_{Nd} record of hydrothermal sediments has the potential for yielding important new information concerning the history of deepwater circulation patterns in the oceans.

[45] **Acknowledgments.** V.C. is funded by the 2000 Southampton Oceanography Centre, fellowship. Hydrothermal research at NOCS is funded through NERC core strategic science. The authors would like to thank two anonymous referees and Jerry Dickens for their insightful comments in improving the manuscript.

References

Abouchami, W., and S. L. Goldstein (1995), A lead isotopic study of circum-Antarctic manganese nodules, *Geochim. Cosmochim. Acta*, *59*, 1809–1820.

Abouchami, W., et al. (1997), Secular changes of lead and neodymium in central Pacific seawater recorded by a Fe-Mn crust, *Geochim. Cosmochim. Acta*, *61*, 3957–3974.

Abouchami, W., et al. (1999), Pb and Nd isotopes in NE Atlantic Fe-Mn crusts: Proxies for trace metal paleosources and paleocean circulation, *Geochim. Cosmochim. Acta*, *63*, 1489–1505.

Albarède, F., et al. (1998), A Hf-Nd isotopic correlation in ferromanganese nodules, *Geophys. Res. Lett.*, *25*, 3895–3898.

Arimoto, R., et al. (1995), Trace elements in the atmosphere over the North Atlantic, *J. Geophys. Res.*, *100*, 1199–1213.

Balsam, W. L., B. L. Otto-Bliesner, and B. C. Deaton (1995), Modern and Last Glacial Maximum eolian sedimentation patterns in the Atlantic Ocean interpreted from sediment iron oxide content, *Paleoceanography*, *10*, 493–507.

Bayon, G., et al. (2002), An improved method for extracting marine sediment fractions and its application to Sr and Nd isotopic analysis, *Chem. Geol.*, *187*, 179–199.

Bayon, G., et al. (2004), Sedimentary Fe-Mn oxyhydroxides as paleoceanographic archives and the role of aeolian flux in regulating oceanic dissolved REE, *Earth Planet. Sci. Lett.*, *224*, 477–492.

Burton, K. W., and D. Vance (2000), Glacial-interglacial variations in the neodymium isotope composition of seawater in the Bay of Bengal recorded by planktonic foraminifera, *Earth Planet. Sci. Lett.*, *176*, 425–441.

Cave, R. R. (2002), A geochemical study of hydrothermal signals in marine sediments: The Rainbow hydrothermal area, 36°N on the Mid-Atlantic Ridge, Ph.D. thesis, 141 pp, Univ. of Southampton, Southampton, U. K.

Cave, R. R., et al. (2002), Fluxes to sediments underlying the Rainbow hydrothermal plume at 36°14′N on the Mid-Atlantic Ridge, *Geochim. Cosmochim. Acta*, *66*, 1905–1923.

Charlou, J. L., et al. (2002), Geochemistry of high H_2 and CH_4 vent fluids issuing from ultramafic rocks at the Rainbow hydrothermal field (36°14′N, MAR), *Chem. Geol.*, *191*, 345–359.

Chavagnac, V., et al. (2005), Sources of REE in sediment cores from the Rainbow vent site (36°14′N, MAR), *Chem. Geol.*, *216*, 329–352.

David, K., et al. (2001), The Hf isotope composition of global seawater and the evolution of Hf isotopes in the deep Pacific Ocean from Fe-Mn crusts, *Chem. Geol.*, *178*, 23–42.

Douville, E., et al. (2002), The Rainbow vent fluids (36°14′N, MAR): The influence of ultramafic rocks and phase separation on trace metal content in Mid-Atlantic Ridge hydrothermal fluids, *Chem. Geol.*, *184*, 37–48.

Dymond, J., and S. Roth (1988), Plume dispersed hydrothermal particles: A time series record of settling flux from the Endeavour Ridge using moored sensors, *Geochim. Cosmochim. Acta*, *52*, 2525–2536.

Edmond, J. M., et al. (1982), Chemistry of hot springs on the East Pacific Rise and their effluent dispersal, *Nature*, *297*, 187–199.

Edmonds, H. N., and C. R. German (2004), Particle geochemistry in the Rainbow hydrothermal plume, Mid-Atlantic Ridge, *Geochim. Cosmochim. Acta*, *68*, 759–772.

Elderfield, H., and M. J. Greaves (1982), The rare earth elements in seawater, *Nature*, *296*, 214–219.

Elderfield, H., et al. (1981), Rare earth element geochemistry of oceanic ferromanganese nodules and associated sediments, *Geochim. Cosmochim. Acta*, *54*, 971–991.

Feely, R. A., et al. (1990), The effect of hydrothermal processes on mid-water phosphorous distributions in the northeast Pacific, *Earth Planet. Sci. Lett.*, *96*, 305–318.

Feely, R. A., G. J. Massoth, E. T. Baker, G. T. Lebon, and T. L. Geiselman (1992), Tracking the dispersal of hydrothermal plumes from the Juan de Fuca Ridge using suspended matter composition, *J. Geophys. Res.*, *97*, 3457–3468.

Feely, R. A., et al. (1994), Hydrothermal plumes along the East Pacific Rise, 8°40′ to 11°50′N: Particle distribution and composition, *Earth Planet. Sci. Lett.*, *128*, 19–36.

Fouquet, Y., et al. (1997), Discovery and first submersible investigations on the Rainbow hydrothermal field on the MAR (36°14′N), *Eos Trans. AGU*, *78*(46), Fall Meet. Suppl., F832.

Frank, M. (2002), Radiogenic isotopes: Traverse of past ocean circulation and erosional input, *Rev. Geophys.*, *40*(1), 1001, doi:10.1029/2000RG000094.

Frank, M., et al. (1999), Nd and Pb isotopes in Atlantic and Pacific water masses before and after closure of the Panam gateway, *Geology*, *27*, 1147–1150.

Gana, S., and C. Provost (1993), Circulation and fluxes of the central North Atlantic in 1983–1984 estimated by inverse analysis of "Topogulf" hydrographic data, *J. Mar. Syst.*, *4*, 67–92.

German, C. R., and K. L. Von Damm (2003), Hydrothermal processes, in *Treatise on Geochemistry*, edited by K. K. Turekian and H. D. Holland, vol. 6, *The Oceans and Marine Geochemistry*, edited by H. Elderfield, pp. 181–222, Elsevier, New York.

German, C. R., et al. (1990), Hydrothermal scavenging of rare earth elements in the ocean, *Nature*, *345*, 516–518.

German, C. R., et al. (1991), Hydrothermal scavenging at the Mid Atlantic Ridge: Modification of trace element dissolved fluxes, *Earth Planet. Sci. Lett.*, *107*, 101–114.

German, C. R., G. P. Klinkhammer, and M. D. Rudnick (1996), The Rainbow hydrothermal plume, 36°15′N, *Geophys. Res. Lett.*, *23*, 2979–2982.

German, C. R., et al. (1998), Topographic control of a dispersing hydrothermal plume, *Earth Planet. Sci. Lett.*, *156*, 267–273.

German, C. R., et al. (2002), Hydrothermal plume-particle fluxes at 13°N on the East Pacific Rise, *Deep Sea Res., Part I*, *49*, 1921–1940.

Godfrey, L. V., et al. (1997), The Hf isotopic composition of ferromanganese nodules and crusts and hydrothermal manganese deposits: Implications for seawater Hf, *Earth Planet. Sci. Lett.*, *151*, 91–105.

Goldberg, E. D., M. Koide, R. A. Schmitt, and R. H. Smith (1963), Rare earth distributions in the marine environment, *J. Geophys. Res.*, *68*, 4209–4217.

Haley, B. A., et al. (2004), Rare earth elements in pore waters of marine sediments, *Geochim. Cosmochim. Acta*, *68*, 1265–1279.

Halliday, A. N., J. P. Davidson, P. Holden, R. M. Owen, and A. M. Olivarez (1992), Metalliferous sediments and the scavenging residence time of Nd near hydrothermal vents, *Geophys. Res. Lett.*, *19*, 761–764.

Holm, N. G., and J. P. Charlou (2001), Initial indications of abiotic formation of hydrocarbon in the Rainbow ultramafic hydrothermal systems Mid-Atlantic Ridge, *Earth Planet. Sci. Lett.*, *191*, 1–8.

Jeandel, C. (1993), Concentration and isotopic composition of Nd in the southern Atlantic Ocean, *Earth Planet. Sci. Lett.*, *117*, 581–591.

Khripounoff, A., and P. Alberic (1991), Settling particles in hydrothermal vent field (East Pacific Rise 13°N) measured by sediment traps, *Deep Sea Res., Part I*, *38*, 729–744.

Klinkhammer, G. P., and M. R. Palmer (1991), Uranium in the oceans: Where it goes and why, *Geochim. Cosmochim. Acta*, *55*, 1799–1806.

Kuss, J., and K. Kremling (1999), Particulate trace element fluxes in the deep northeast Atlantic Ocean, *Deep Sea Res., Part I*, *46*, 149–169.

Lacan, F. (2002), Masses d'eau des mers nordiques et de l'Atlantique subarctique tracées par les isotopes du néodyme, Ph.D. thesis, Univ. Paul Sabatier Toulouse III, Toulouse, France.

Lacan, F., and C. Jeandel (2001), Tracing Papua New Guinea imprint on the central equatorial Pacific Ocean using neodymium isotopic compositions and rare earth element patterns, *Earth Planet. Sci. Lett.*, *186*, 497–512.

Lacan, F., and C. Jeandel (2005a), Neodymium isotopes as a new tool for quantifying exchange fluxes at the continent-ocean interface, *Earth Planet. Sci. Lett.*, *232*, 245–257.

Lacan, F., and C. Jeandel (2005b), Acquisition of the neodymium isotopic composition of the North Atlantic Deep Water, *Geochem. Geophys. Geosyst.*, *6*, Q12008, doi:10.1029/2005GC000956.

Lilley, M. D. et al. (1995), Chemical and biochemical transformations in hydrothermal systems, in *Seafloor Hydrothermal Systems: Physical, Chemical, Biological and Geological Interactions*, *Geophys. Monogr. Ser.*, vol. 91, edited by S. E. Humpris et al., pp. 369–391, AGU, Washington, D. C.

Ling, H. F., et al. (1997), Evolution of Nd and Pb isotopes in central Pacific seawater from ferromanganese crusts, *Earth Planet. Sci. Lett.*, *146*, 1–12.

Ludford, E. M., M. R. Palmer, C. R. German, and G. P. Klinkhammer (1996), The geochemistry of Atlantic hydrothermal particles, *Geophys. Res. Lett.*, *23*, 3503–3506.

Lunel, T., et al. (1990), Aluminum as a depth-sensitive tracer of entrainment in submarine hydrothermal plumes, *Nature*, *344*, 137–139.

Marques, A. F. A., et al. (2006), Mineralogy, geochemistry and Nd isotopes of the Rainbow hydrothermal field, Mid-Atlantic Ridge, *Mineral. Deposita*, *41*, 52–67.

McLennan, S. M. (1989), Rare earth elements in sedimentary rocks: Influence of provenance and sedimentary processes, in *Geochemistry and Mineralogy of Rare Earth Elements*, edited by B. R. Lipin and G. A. McKay, *Rev. Mineral.*, *21*, 169–200.

Metz, S., and J. H. Trefry (1993), Field and laboratory studies of metal uptake and release by hydrothermal precipitates, *J. Geophys. Res.*, *98*, 9661–9666.

Millero, F. J. (1996), *Chemical Oceanography*, 469 pp., CRC Press, Boca Raton, Fla.

Mills, R. A., et al. (2001), Genesis of ferromanganese crusts from the TAG hydrothermal field, *Chem. Geol.*, *176*, 283–293.

Olivarez, A. M., and R. M. Owen (1989), REE/Fe variations in hydrothermal sediments: Implications for the REE content of seawater, *Geochim. Cosmochim. Acta*, *53*, 757–762.

Owen, R. M., and A. M. Olivarez (1988), Geochemistry of rare earth elements in Pacific hydrothermal sediments, *Mar. Chem.*, *25*, 183–196.

Palmer, M. R. (1985), Rare earth elements in foraminifera tests, *Earth Planet. Sci. Lett.*, *73*, 285–298.

Palmer, M. R., and H. Elderfield (1985), Variations in the Nd isotopic composition of foraminifera from Atlantic Ocean sediments, *Earth Planet. Sci. Lett.*, *73*, 299–305.

Patchett, P. J., et al. (1984), Hafnium/rare earth element fractionation in the sedimentary system and crustal recycling into the Earth's mantle, *Earth Planet. Sci. Lett.*, *69*, 365–378.

Piepgras, D. J., and G. J. Wasserburg (1987), Rare earth element transport in the western North Atlantic inferred from isotopic observations, *Geochim. Cosmochim. Acta*, *51*, 1257–1271.

Piepgras, D. J., et al. (1979), The isotopic composition of Nd in different ocean masses, *Earth Planet. Sci. Lett.*, *45*, 223–236.

Piotrowski, A. N., et al. (2000), Changes in erosion and ocean circulation recorded in the Hf isotopic compositions of North Atlantic and Indian Ocean ferromanganese crusts, *Earth Planet. Sci. Lett.*, *181*, 315–325.

Piotrowski, A. M., et al. (2004), Intensification and variability of ocean thermohaline circulation through the last deglaciation, *Earth Planet. Sci. Lett.*, *225*, 205–220.

Piotrowski, A. M., et al. (2005), Temporal relationships of carbon cycling and ocean circulation at glacial boundaries, *Science*, *307*, 1933–1938.

Pomies, C., et al. (2002), Neodymium in modern foraminifera from the Indian Ocean: Implications for the use of foraminiferal Nd isotope compositions in paleoceanography, *Earth Planet. Sci. Lett.*, *203*, 1031–1045.

Reynolds, B. C., et al. (1999), Nd- and Pb- isotope time series from Atlantic ferromanganese crusts: Implications for changes in provenance and paleo-circulation over the last 8 Myr, *Earth Planet. Sci. Lett.*, *173*, 381–396.

Ruhlin, D. E., and R. M. Owen (1986), The rare earth element geochemistry of hydrothermal sediments from the East Pacific Rise: Examination of a seawater scavenging mechanism, *Geochim. Cosmochim. Acta*, *50*, 393–400.

Rutberg, R. L., et al. (2000), Reduced North Atlantic Deep Water flux to the glacial Southern Ocean inferred from neodymium isotope ratios, *Nature*, *405*, 935–938.

Sarnthein, M., et al. (1994), Changes in east Atlantic deepwater circulation over the last 30,000 years: Eight time slice reconstructions, *Paleoceanography*, *9*, 209–267.

Saunders, P. M. (1982), Circulation in the eastern North Atlantic, *J. Mar. Res.*, *40*, 641–657.

Schaller, T., et al. (2000), Oxyanions in metalliferous sediments: Tracers for paleowater metal concentrations?, *Geochim. Cosmochim. Acta*, *63*, 2243–2254.

Schmitz, W. J. J. (1996), On the world ocean circulation, vol. I, *Tech. Rep. WHOI-96–03*, 141 pp., Woods Hole Oceanogr. Inst., Woods Hole, Mass.

Severmann, S., et al. (2004), The origin of clay minerals in active and relict hydrothermal deposits, *Geochim. Cosmochim. Acta*, *68*, 73–88.

Seyfried, W. E. Jr., D. I. Foustoukos, and D. E. Allen (2004), Ultramafic-hosted hydrothermal systems at mid-ocean ridges: Chemical and physical controls on pH, redox and carbon reductions reactions, in *Mid-Ocean Ridges: Hydrothermal Interactions Between the Lithosphere and Oceans*, *Geophys. Monogr. Ser.*, vol. 148, edited by C. R. German, J. Lin, and L. Parson, pp. 267–284, AGU, Washington D. C.

Sherrell, R. M., et al. (1999), Uptake and fractionation of rare earth elements on hydrothermal plume particles at 9°45′N, East Pacific Rise, *Geochim. Cosmochim. Acta*, *63*, 1709–1722.

Sholkovitz, E. R. (1992), Chemical evolution of rare earth elements: Fractionation between colloidal and solution phases of filtered river water, *Earth Planet. Sci. Lett.*, *114*, 77–84.

Spivack, A. J., and G. J. Wasserburg (1988), Neodymium isotopic composition of the Mediterranean outflow and the eastern North Atlantic, *Geochim. Cosmochim. Acta*, *52*, 2767–2773.

Sverjensky, D. A. (1984), Europium redox equilibria in aqueous solution, *Earth Planet. Sci. Lett.*, *67*, 70–78.

Tachikawa, K., et al. (1997), Distribution of rare earth elements and neodynium isotopes in settling particulate material of the tropical Atlantic Ocean (EUMELI site), *Deep Sea Res., Part I*, *44*(11), 1769–1792.

Tachikawa, K., et al. (1999), A new approach to the Nd residence time in the ocean: The role of the atmospheric inputs, *Earth Planet. Sci. Lett.*, *170*, 433–446.

Thurnherr, A. M., and K. J. Richards (2001), Hydrography and high-temperature heat flux of the Rainbow hydrothermal site (36°14′N, Mid-Atlantic Ridge), *J. Geophys. Res.*, *106*, 9411–9426.

Thurnherr, A. M., et al. (2002), Flow and mixing in the rift valley of the Mid-Atlantic Ridge, *J. Phys. Oceanogr.*, *132*, 1763–1778.

Trefry, J. H., and S. Metz (1989), Role of hydrothermal precipitates in the geochemical cycling of vanadium, *Nature*, *342*, 531–533.

Turner, D. R., and M. Whitfield (1979), Control of seawater composition, *Nature*, *281*, 468–469.

Van Aken, H. M. (2000), The hydrography of the mid-latitude northeast Atlantic Ocean I: The deep water masses, *Deep Sea Res., Part I*, *47*, 757–788.

Van Aken, H. M., and G. Becker (1996), Hydrography and through-flow in the north-eastern North Atlantic Ocean: The NANSEN project, *Prog. Oceanogr.*, *38*, 297–346.

Vance, D., and K. W. Burton (1999), Neodynium isotopes in planktonic foraminifera: A record of the response of continental weathering and ocean circulation rates to climate change, *Earth Planet. Sci. Lett.*, *173*, 365–379.

Vance, D., A. E. Scrivner, P. Beney, M. Staubwasser, G. M. Henderson, and N. C. Slowey (2004), The use of foraminifera as a record of the past neodymium isotope composition of seawater, *Paleoceanography*, *19*, PA2009, doi:10.1029/2003PA000957.

van de Flierdt, T., et al. (2002), Glacial weathering and the hafnium isotope composition of seawater, *Earth Planet. Sci. Lett.*, *201*, 639–647.

van de Flierdt, T., et al. (2004a), New constraints on the sources and behavior of neodymium and hafnium in seawater from the Pacific Ocean ferromanganese crusts, *Geochim. Cosmochim. Acta*, *68*, 3827–3843.

van de Flierdt, T., M. Frank, A. N. Halliday, J. R. Hein, B. Hattendorf, D. Günther, and P. W. Kubik (2004b), Deep and bottom water export from the Southern Ocean to the Pacific over the past 38 million years, *Paleoceanography*, *19*, PA1020, doi:10.1029/2003PA000923.

Veizer, J., et al. (1999), $^{87}Sr/^{86}Sr$, $\partial^{13}C$ and $\partial^{18}O$ evolution of Phanerozoic seawater, *Chem. Geol.*, *161*, 59–88.

Vlastélic, I., et al. (2001), Geographic control on Pb isotope distribution and sources in Indian Ocean Fe-Mn deposits, *Geochim. Cosmochim. Acta*, *65*, 4303–4319.

Watkins, S. J., and B. A. Maher (2003), Magnetic characterization of present-day deep-sea sediments and sources in the North Atlantic, *Earth Planet. Sci. Lett.*, *214*, 379–394.

White, W. M., et al. (1986), Hf isotope ratios of marine sediments and Mn nodules: Evidences for mantle source of Hf in seawater, *Earth Planet. Sci. Lett.*, *79*, 46–54.

Wilson, T. R. S., et al. (1985), Early organic diagenesis: The significance of progressive subsurface oxidation fronts in pelagic sediments, *Geochim. Cosmochim. Acta*, *49*, 811–822.

V. Chavagnac and D. R. H. Green, National Oceanography Centre, Southampton, University of Southampton, Waterfront Campus, European Way, Southampton SO14 3ZH, UK. (vmcc@noc.soton.ac.uk)

C. R. German, Department of Geology and Geophysics, Woods Hole Oceanographic Institution, Woods Hole, MA 02543, USA.

J. A. Milton and M. R. Palmer, School of Ocean and Earth Sciences, University of Southampton, Waterfront Campus, European Way, Southampton SO14 3ZH, UK.